clude investigations of output coupling of the molecules from the condensate, the formation of other bound states, and the dependence of the molecule-condensate interactions on the ro-vibrational state of the molecule. The binding energies of the highest 5 to 10 vibrational bound states could be measured to a precision of about 10^{-7} cm^{-1}, which would provide extremely precise information on the long-range atomic interactions. The molecular cloud might be directly imaged. It should be possible to realize the limit in which the stimulated transition rate exceeds the molecular decay rate (*8*). In this regime, reversible formation of a molecular Bose condensate from an atomic condensate could occur (*5*–*8*), and further studies of mixed atom-molecular condensates and nonlinear matter wave phenomena would be feasible.

References and Notes

1. M. H. Anderson *et al.*, *Science* **269**, 198 (1995).
2. C. C. Bradley *et al.*, *Phys. Rev. Lett.* **75**, 1687 (1995); K. B. Davis *et al.*, *Phys. Rev. Lett.* **75**, 3969 (1995).
3. M. Inguscio, S. Stringari, C. E. Wieman, Eds., *Bose-Einstein Condensation in Atomic Gases*, Proceedings of the 1998 Enrico Fermi Summer School, Course CXL (IOS Press, Amsterdam, 1999).
4. E. A. Burt *et al.*, *Phys. Rev. Lett.* **79**, 337 (1997); D. M. Stamper-Kurn *et al.*, *Phys. Rev. Lett.* **80**, 2027 (1998).
5. P. D. Drummond, K. V. Kheruntsyan, H. He, *Phys. Rev. Lett.* **81**, 3055 (1998).
6. J. Javanainen and M. Mackie, *Phys. Rev. A* **59**, R3186 (1999).
7. E. Timmermans *et al.*, *Phys. Rev. Lett.* **83**, 2691 (1999).
8. D. J. Heinzen, R. H. Wynar, P. D. Kheruntsyan, P. D. Drummond, unpublished results.
9. P. S. Julienne *et al.*, *Phys. Rev. A* **58**, R797 (1998).
10. E. R. I. Abraham *et al.*, *Phys. Rev. Lett.* **74**, 1315 (1995).
11. C. C. Tsai *et al.*, *Phys. Rev. Lett.* **79**, 1245 (1997).
12. A. Fioretti *et al.*, *Phys. Rev. Lett.* **80**, 4402 (1998); A. N. Nikolov *et al.*, *Phys. Rev. Lett.* **82**, 703 (1999); T. Takekoshi *et al.*, *Phys. Rev. A* **59**, R5 (1999).
13. S. Inouye *et al.*, *Nature* **392**, 151 (1998); Ph. Courteille *et al.*, *Phys. Rev. Lett.* **81**, 69 (1998); J. L. Roberts *et al.*, *Phys. Rev. Lett.* **81**, 5109 (1998); V. Vuletić *et al.*, *Phys. Rev. Lett.* **82**, 1406 (1999).
14. D. J. Han *et al.*, *Phys. Rev. A* **57**, R4114 (1998).
15. J. R. Gardner *et al.*, *Phys. Rev. Lett.* **74**, 3764 (1995); H. M. J. M. Boesten *et al.*, *J. Phys. B* **32**, 287 (1999).
16. N. Balakrishnan *et al.*, *Chem. Phys. Lett.* **280**, 5 (1997).
17. F. A. Van Abeelen and B. J. Verhaar, *Phys. Rev. Lett.* **83**, 1550 (1999); V. A. Yurovsky *et al.*, *Phys. Rev. A* **60**, R765 (1999).
18. J. M. Vogels *et al.*, *Phys. Rev. A* **56**, R1067 (1997); P. S. Julienne *et al.*, *Phys. Rev. Lett.* **78**, 1880 (1997).
19. F. Dalfovo *et al.*, *Rev. Mod. Phys.* **71**, 463 (1999).
20. D. G. Fried *et al.*, *Phys. Rev. Lett.* **81**, 3811 (1998).
21. J. L. Bohn and P. S. Julienne, *Phys. Rev. A* **60**, 414 (1999).
22. N. Balakrishnan *et al.*, *Phys. Rev. Lett.* **80**, 3224 (1998).
23. R. C. Forrey *et al.*, *Phys. Rev. A* **58**, R2645 (1998); R. C. Forrey *et al.*, *Phys. Rev. Lett.* **82**, 2657 (1999).

24. We gratefully acknowledge support by NSF, the R. A. Welch Foundation, and the NASA Microgravity Research Division.

12 November 1999; accepted 13 December 1999

Zener Model Description of Ferromagnetism in Zinc-Blende Magnetic Semiconductors

T. Dietl,[1,2]* H. Ohno,[1]* F. Matsukura,[1] J. Cibert,[3] D. Ferrand[3]

Ferromagnetism in manganese compound semiconductors not only opens prospects for tailoring magnetic and spin-related phenomena in semiconductors with a precision specific to III-V compounds but also addresses a question about the origin of the magnetic interactions that lead to a Curie temperature (T_C) as high as 110 K for a manganese concentration of just 5%. Zener's model of ferromagnetism, originally proposed for transition metals in 1950, can explain T_C of $Ga_{1-x}Mn_xAs$ and that of its II-VI counterpart $Zn_{1-x}Mn_xTe$ and is used to predict materials with T_C exceeding room temperature, an important step toward semiconductor electronics that use both charge and spin.

Advances in the epitaxy of III-V semiconductor compounds now make it possible to fabricate quantum structures in which confined electrons or photons exhibit outstanding properties and functionalities. The atomic precision of deposition and processing has made it possible to observe and examine quantum Hall effects, dot and microcavity semiconductor lasers, and single-electron charging phenomena, to name only a few from many other recent developments (*1*). Therefore, the discovery of ferromagnetism in (In,Mn)As (*2*) and then in (Ga,Mn)As (*3*) enables examination of collective magnetic phenomena in a well-controlled environment. At the same time, applications in sensors and memories as well as for computing with electron spins can be envisaged (*4*). It is then important to understand the ferromagnetism in these semiconductors and to ask whether the T_C's can be raised to above 300 K from the present 110 K (*3*).

Our theory considers ferromagnetic correlation mediated by holes originating from shallow acceptors in the ensemble of the localized spins in doped magnetic semiconductors. The magnetic ion Mn, which occupies the cation (Ga) sublattice in zinc-blende $Ga_{1-x}Mn_xAs$ (*5*), provides a localized spin and at the same time acts as an acceptor. These Mn acceptors compensate the deep antisite donors commonly present in GaAs grown by low-temperature molecular beam epitaxy and produce a p-type conduction with metallic resistance for the Mn concentration x in the range $0.04 \le x \le 0.06$ (*6*, *7*). According to optical studies, Mn in GaAs forms an acceptor center characterized by a moderate binding energy (*8*), $E_a = 110$ meV, and a small magnitude of the energy difference between the triplet and singlet state of the bound hole (*8*, *9*), $\Delta\varepsilon = 8 \pm 3$ meV. This value demonstrates that the hole introduced by the divalent Mn does not occupy d shell or form a Zhang-Rice–like singlet (*10*) so that, despite a strong p-d hybridization, (Ga,Mn)As can be classified as a charge-transfer insulator, a conclusion confirmed by photoemission spectroscopy (*11*).

Zener (*12*) first proposed the model of ferromagnetism driven by the exchange interaction between carriers and localized spins. However, this model was later abandoned, as neither the itinerant character of the magnetic electrons nor the quantum (Friedel) oscillations of the electron spin polarization around the localized spins were taken into account; both of these are now established to be critical ingredients for the theory of magnetic metals. We emphasize that in the case of semiconductors, however, the effect of the Friedel oscillations averages to zero because the mean distance between the carriers is greater than that between the spins. In such a case, the Zener model becomes equivalent (*13*) to the approach developed by Ruderman, Kittel, Kasuya, and Yosida (RKKY), in which the presence of the oscillations is taken explicitly into account.

We began by determining how the Ginzburg-Landau free-energy functional F depends on the magnetization M of the localized spins. In the case of the holes residing in the Γ_8 valence bands, spin-orbit coupling and the kp interaction, that is, the mixing of the angular momentum basis states associated with the delocalization of atomic orbitals, are expected to play an important role. Therefore, we computed the carrier contribution to F, $F_c[M]$, by diagonalizing the 6×6 Kohn-Luttinger matrix (*14*) together with the p-d exchange contribution (*15*) and by integrating over the rather anisotropic Fermi volume (inset, Fig. 1). The model allows for the presence of strain and arbitrary orientations of M. Standard values of the Luttinger parameters γ_i and the spin-orbit splitting Δ_o were taken as input parameters (*16*). Ac-

[1]Research Institute of Electrical Communication, Tohoku University, Katahira 2-1-1, Sendai 980-8577, Japan. [2]Institute of Physics and College of Science, Polish Academy of Sciences, al. Lotników 32/46, PL-02668 Warsaw, Poland. [3]Laboratoire de Spectrométrie Physique, Université Joseph Fourier Grenoble 1-CNRS (UMR 5588), F-38402 Saint Martin d'Hères Cedex, France.

*To whom correspondence should be addressed. E-mail: dietl@ifpan.edu.pl; ohno@riec.tohoku.ac.jp

cording to interband magneto-optics (*17*) and photoemission studies (*11*), $\beta N_o = -1.1 \pm 0.1$ and -1.2 ± 0.2 eV for (Zn,Mn)Te and (Ga,Mn)As, respectively. Here β is the p-d exchange integral and N_o is the concentration of cation sites. Like other thermodynamic quantities, $F_c[M]$ is expected to be weakly perturbed by static disorder, whereas its enhancement by the effects of carrier-carrier interactions can be described by the Fermi-liquid parameter A_F. The value of $A_F = 1.2$, as evaluated (*18*) by the local spin density approximation for the relevant hole concentrations, is adopted here.

The remaining part of the free-energy functional, that of the localized spins, is given by

$$F_S[M] = -\int_0^M dM_o H(M_o) \qquad (1)$$

where $H(M_o)$ is the inverse function of the experimental dependence of the magnetization on the magnetic field H in the absence of the carriers. This dependence is conveniently parameterized by the Brillouin function, in which two empirical parameters, the effective spin concentration $x_{eff}N_o < xN_o$ and temperature $T_{eff} > T$, account for the presence of antiferromagnetic superexchange interactions (*17*, *19*, *20*). Accordingly, x_{eff} determines the magnitude of the Curie constant, and the antiferromagnetic temperature $T_{AF} = T_{eff} - T$ describes the contribution of the antiferromagnetic interactions to the Curie-Weiss temperature. The dependencies $x_{eff}(x)$ and $T_{AF}(x)$ are known (*17*, *19*) for (Zn,Mn)Te, whereas $x \approx x_{eff}$ and $T_{AF} \approx 0$ for (Ga,Mn)As, as explained later. By minimizing $F_c[M] + F_S[M]$ with respect to M at given T and hole concentration p, we obtain T_C within the mean-field approximation, an approach that is quantitatively valid for long-range exchange interactions.

The above model implies that the Curie temperature is determined by a competition between the ferromagnetic and antiferromagnetic interactions, $T_C = T_F - T_{AF}$. The normalized ferromagnetic temperature T_F^{nor}, from which the expected magnitude of the Curie temperature can be calculated according to

$$T_C(x) = A_F(x_{eff}/0.05)(\beta N_o[\text{eV}])^2 [N_o(\text{GaAs})/N_o]T_F^{nor} - T_{AF}(x) \qquad (2)$$

is shown for p-(Ga,Mn)As and p-(Zn,Mn)Te (Fig. 1). The results confirm an expected strong dependence of T_C on x and p. At a given p, the magnitude of T_F^{nor} is substantially greater in the case of p-(Ga,Mn)As. This is mainly caused by the smaller value of the spin-orbit splitting between the Γ_8 and Γ_7 bands in arsenides, $\Delta_o = 0.34$ eV, in comparison with that of tellurides, $\Delta_o = 0.91$ eV, a chemical trend confirmed in Fig. 3. Once the Fermi energy ε_F approaches the Γ_7 band, the density-of-states effective mass increases, and the reduction of the carrier spin susceptibility by the spin-orbit interaction is diminished. The computed value of T_F^{nor} for $p = 3 \times 10^{20}$ cm^{-3} is greater by a factor of 4 in (Ga,Mn)As than that evaluated in the limit $\Delta_o \gg \varepsilon_F$.

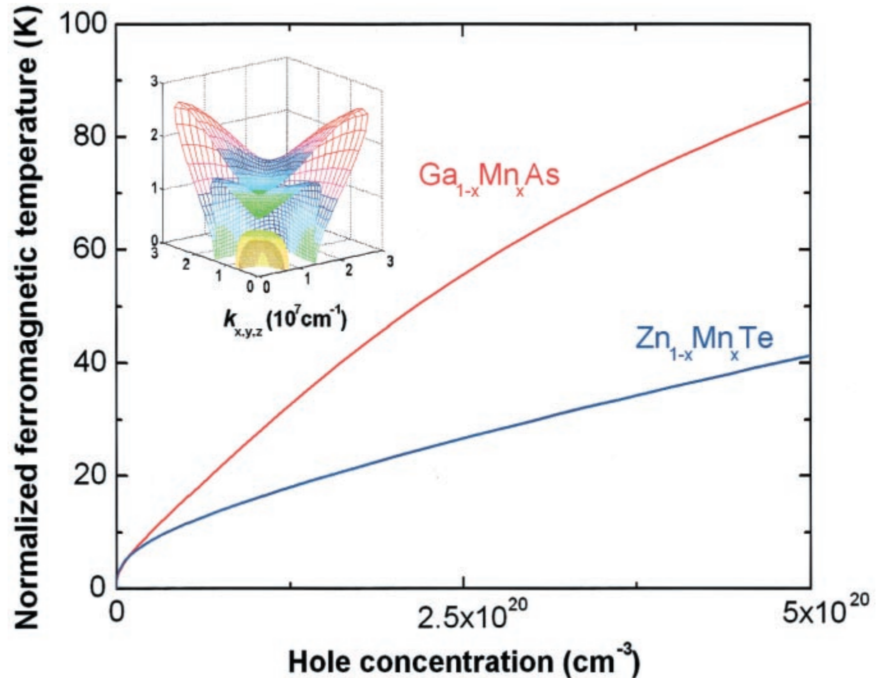

Fig. 1. Normalized ferromagnetic temperature T_F^{nor} as a function of hole concentration. Inset shows an example of the cross section of the Fermi volume of holes in a ferromagnetic zinc-blende semiconductor: Nonzero magnetization leads to a splitting of the valence band into four subbands. This complex valence-band structure was used to determine the mean-field values of T_F^{nor} for p-$Ga_{0.95}Mn_{0.05}As$ and p-$Zn_{0.95}Mn_{0.05}Te$ (solid lines) and to establish the chemical trends depicted in Fig. 3.

Because of the large T_C, the spin-dependent extraordinary contribution to the Hall resistance R_H in (Ga,Mn)As persists up to 300 K, making an accurate determination of the hole density difficult (*6*, *7*). However, the recent measurement (*21*) of R_H up to 27 T and at 50 mK yielded an unambiguous value of $p = 3.5 \times 10^{20}$ cm^{-3} for a metallic $Ga_{0.947}Mn_{0.053}As$ sample, in which $T_C = 110$ K is observed (*3*). This agrees with the computed value $T_C = 120$ K.

The studied layers of (Zn,Mn)Te:N are on the insulating side of the metal-insulator transition (MIT), as the bound magnetic polaron (BMP) formation enhances localization; the effect of the MIT on magnetism is discussed below. Nevertheless, the comparison of the experimental (*22*) and calculated values of T_C for (Zn,Mn)Te as a function of x and p (Fig. 2) shows that the model explains the magnitude of T_C except for the samples with the smallest x. In the case of the sample with the lowest Mn content x, p/xN_o is as large as 0.6 so that precursor effects of Friedel oscillations and Kondo correlation are expected at low temperatures (*13*).

An important aspect of the present model is that it takes into account the anisotropy of the carrier-mediated exchange interaction associated with the spin-orbit coupling in the host material, an effect difficult to take into account within the standard approach to the RKKY interaction. Although the anisotropy associated with epitaxial strain has a minor influence on T_C in (Ga,Mn)As [on the order of 1 K for 1% biaxial strain in the (001) plane], the strain drastically affects the orientation of the easy axis. Although the easy axis is along [110] in the case of unstrained or compressively strained films for the relevant hole concentrations, under tensile strain, the easy axis takes the [001] direction. These predictions are corroborated by available experimental data (*3*).

The agreement between experiment and theory for T_C and the magnetic anisotropy demonstrates that the present model, developed with no adjustable parameter, explains quantitatively the ferromagnetism observed in (Ga,Mn)As as well as the striking difference between T_C values in (Ga,Mn)As and p-(Zn,Mn)Te. It also suggests that T_C values above 300 K could be achieved in $Ga_{0.9}Mn_{0.1}As$ if such a large value of x could be accompanied by a corresponding increase of p.

As the carriers are known to be at the localization boundary in the present semiconductor systems, it is important to discuss the effect of localization on the onset of ferromagnetism. The two-fluid model (*23*) constitutes the established description of electronic states in the vicinity of the Anderson-Mott MIT in doped

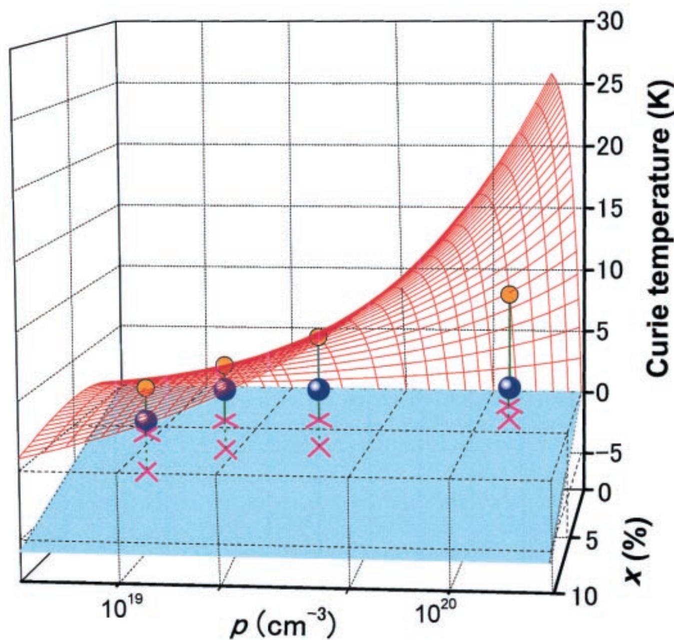

Fig. 2. Curie temperature T_C in $Zn_{1-x}Mn_xTe$:N for various Mn contents x and hole concentrations p deduced from the Hall resistance at 300 K. The plane with upper crosses corresponds to $T_C = 0$. Experimental values are marked by blue spheres (*22*) and theoretical predictions by the red mesh and attached yellow spheres. According to Eq. 2, T_C is determined by a competition between the hole-induced ferromagnetic interactions (characterized by T_{Fnor} depicted in Fig. 1) and the antiferromagnetic interactions, described by $-T_{AF}$, shown by the plane with lower crosses.

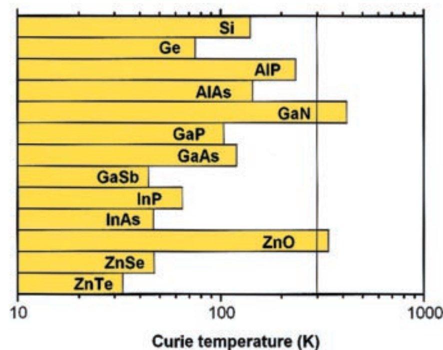

Fig. 3. Computed values of the Curie temperature T_C for various p-type semiconductors containing 5% of Mn and 3.5×10^{20} holes per cm^3.

semiconductors. According to that model, the conversion of itinerant electrons into singly occupied impurity states with increasing disorder occurs gradually and has already begun on the metal side of the MIT. This leads to a disorder-driven static phase separation into two types of regions: one populated by electrons in extended states and another containing singly occupied impurity-like states. The latter controls the magnetic response of doped nonmagnetic semiconductors (*23*) and gives rise to the presence of BMPs on both sides of the MIT in magnetic semiconductors (*20*). On crossing the MIT, the extended states become localized. However, according to the scaling theory of the MIT, their localization radius ξ decreases rather gradually from infinity at the MIT toward the Bohr radius deep in the insulator phase, so that on a length scale smaller than ξ, the wave function retains an extended character. Such weakly localized states are thought to determine the static longitudinal and Hall conductivities of doped semiconductors.

We suggest that the holes in the extended or weakly localized states mediate the long-range interactions between the localized spins on both sides of the MIT in the III-V and II-VI magnetic semiconductors. The participation of the same set of holes in both charge transport and the ferromagnetic interactions is shown, in (Ga,Mn)As (*6*) and in (Zn,Mn)Te (*22*), by the agreement between the temperature and field dependences of the magnetization deduced from the extraordinary Hall effect, M_H, and from direct magnetization measurements, M_D, particularly in the vicinity of T_C. However, below T_C and in the magnetic fields greater than the coercive force, while M_H saturates (as in standard ferromagnets), M_D continues to rise with the magnetic field (*6*, *24*). We assign this increase to the BMPs, which interact weakly with the ferromagnetic liquid. To gain the Coulomb energy, the BMPs are preferentially formed around close pairs of ionized acceptors. In the case of p-(Ga,Mn)As, this leads to a local ferromagnetic alignment of neighbor Mn d^5 negative ions (*25*), so that $x \approx x_{eff}$ and $T_{AF} \approx 0$. By contrast, BMPs in p-(Zn,Mn)Te are not preferentially formed around Mn pairs and encompass more Mn spins for a given x, as the small binding energy (*22*) E_a = 54 meV corresponds to a relatively large localization radius.

Finally, the values of T_C computed for various semiconductors containing 5% of Mn and 3.5×10^{20} holes per cm^3 are presented (Fig. 3). In addition to adopting the tabulated values of γ_i and Δ_o (*16*), we assumed the same value of $\beta = \beta$(GaMnAs) for all group IV and III-V compounds, which results in an increase of $\beta N_o \propto a_o^{-3}$, where a_o is the lattice constant, a trend known to be obeyed within the II-VI family of magnetic semiconductors (*15*, *16*). By extending the model for wurzite semiconductors, we evaluated T_C for ZnO (*26*) (Fig. 3) and for wurzite GaN (*27*). For the parameters used (*28*), the T_C value for the cubic GaN (Fig. 3) is 6% greater than that computed for the wurzite structure.

The data (Fig. 3) demonstrate that there is much room for a further increase of T_C in p-type magnetic semiconductors. In particular, a general tendency for greater T_C values in the case of lighter elements stems from the corresponding increase in p-d hybridization and reduction of spin-orbit coupling. We believe that this tendency is not altered by the uncertainties in the values of the relevant parameters. Important issues of solubility limits and self-compensation as well as of the transition to a strong-coupling case with decreasing a_o (*10*) need to be addressed experimentally.

The theoretical model described here of the hole-mediated exchange interactions explicitly takes into account the complex valence-band structure of zinc-blende ferromagnetic semiconductors. Our results reveal the important effect of the spin-orbit coupling in the valence band in determining the magnitude of the T_C and the direction of the easy axis in p-type ferromagnetic semiconductors. This coupling, together with a preferential formation of the magnetic polarons at the Mn pairs, makes the T_C of (Ga,Mn)As an order of magnitude greater than that of (Zn,Mn)Te:N, despite the fact that in both cases the ferromagnetic interactions are mediated by the weakly localized holes. Even higher values of T_C are predicted for materials containing greater concentrations of holes and magnetic ions or consisting of lighter elements.

References and Notes

1. See, for example, S. Das Sarma and A. Pinczuk, Eds., *Perspectives in Quantum Hall Effects* (Wiley, New York, 1997); J. Rarity and C. Weisbuch, *Microcavities and Photonic Bandgaps: Physics and Applications* (Kluwer, Dordrecht, Netherlands, 1996); F. H. Julien and A. Alexandrou, *Science* **282**, 1429 (1998), and references therein.
2. H. Ohno, H. Munekata, T. Penney, S. von Molnár, L. L. Chang, *Phys. Rev. Lett.* **68**, 2664 (1992).
3. H. Ohno *et al.*, in *Proceedings 23rd International Conference on Physics of Semiconductors* (World Scientific, Singapore, 1996), pp. 405–408; H. Ohno *et al.*, *Appl. Phys. Lett.* **69**, 363 (1996).
4. J. Shi, S. Gider, K. Babcock, D. D. Awschalom, *Science* **271**, 937 (1996); H. Ohno, *Science* **281**, 951 (1998); G. A. Prinz, *Science* **282**, 1660 (1998); J. De Boeck and G. Borghs, *Phys. World* (April 1999), p. 27; D. P. DiVincenzo, *J. Appl. Phys.* **85**, 4785 (1999), and references therein.
5. R. Shioda, K. Ando, T. Hayashi, M. Tanaka, *Phys. Rev. B* **58**, 1100 (1998).
6. A. Oiwa *et al.*, *Solid State Commun.* **103**, 209 (1997).
7. A. Van Esch *et al.*, *Phys. Rev. B* **56**, 13103 (1997); F. Matsukura, H. Ohno, A. Shen, Y. Sugawara, *Phys. Rev. B* **57**, R2037 (1998); H. Shimizu, T. Hayashi, T. Nishinaga, M. Tanaka, *Appl. Phys. Lett.* **74**, 398 (1999).
8. M. Linnarsson, E. Janzén, B. Monemar, M. Kleverman, A. Thilderkvist, *Phys. Rev. B* **55**, 6938 (1997).
9. N. S. Averkiev, A. A. Gutkin, E. B. Osipov, M. A. Reshchikov, *Fiz. Tekh. Poluprovodn.* **21**, 1847 (1987) [*Sov. Phys. Semicond.* **21**, 1119 (1987)].

10. C. Benoit à la Guillaume, D. Scalbert, T. Dietl, *Phys. Rev. B* **46**, 9853 (1992).
11. J. Okabayashi *et al.*, *Phys. Rev. B* **58**, R4211 (1998).
12. C. Zener, *Phys. Rev.* **81**, 440 (1950); *Phys. Rev.* **83**, 299 (1950). A similar model for the nuclear ferromagnetism was developed by H. Fröhlich and F. R. N. Nabarro [*Proc. R. Soc. London Ser. A* **175**, 382 (1940)].
13. T. Dietl, A. Haury, Y. Merle d'Aubigné, *Phys. Rev. B* **55**, R3347 (1997).
14. See, for example, G. L. Bir and G. E. Pikus, *Symmetry and Strain-Induced Effects in Semiconductors* (Wiley, New York, 1974).
15. See, for example, J. K. Furdyna, *J. Appl. Phys.* **64**, R29 (1988).
16. D. Bimberg *et al.*, *in Landolt-Börstein, New Series*, vol. 17a, O. Madelung, M. Schulz, W. Weiss, Eds. (Springer-Verlag, Berlin, 1982); I. Broser *et al.*, in *Landolt-Börstein, New Series*, vol. 17b, O. Madelung, M. Schulz, W. Weiss, Eds. (Springer-Verlag, Berlin, 1982); O. Madelung, W. von der Osten, U. Rössler, in *Landolt-Börstein, New Series*, vol. 22a, O. Madelung, Ed. (Springer-Verlag, Berlin, 1987); R. Blachnik *et al.*, in *Landolt-Börstein, New Series*, vol. 41B, U. Rössler, Ed. (Springer-Verlag, Berlin, 1999); I. Stolpe *et al.*, *Physica B* **256–258**, 659 (1998).
17. A. Twardowski, P. Świderski, M. von Ortenberg, R. Pauthenet, *Solid State Commun.* **50**, 509 (1984).
18. T. Jungwirth, W. A. Atkinson, B. H. Lee, A. H. MacDonald, *Phys. Rev. B* **59**, 9818 (1999).
19. Y. Shapira *et al.*, *Phys. Rev. B* **33**, 356 (1986).
20. M. Sawicki *et al.*, *Phys. Rev. Lett.* **56**, 508 (1986); P. Głód, T. Dietl, M. Sawicki, I. Miotkowski, *Physica B* **194-196**, 995 (1994).
21. H. Ohno, F. Matsukura, T. Omiya, N. Akiba, *J. Appl. Phys.* **85**, 4277 (1999).
22. D. Ferrand *et al.*, *J. Crystal Growth*, in press (e-print available at xxx.lanl.gov/abs/cond-mat/9910131).
23. See, for example, M. A. Paalanen and R. N. Bhatt, *Physica B* **169**, 223 (1991).
24. B. Beshoten *et al.*, *Phys. Rev. Lett.* **83**, 3073 (1999).
25. J. Blinowski, P. Kacman, J. A. Majewski, in *High Magnetic Fields in Semiconductor Physics II*, G. Landwehr and W. Ossau, Eds. (World Scientific, Singapore, 1997), pp. 861–864.
26. Parameters of ZnO were obtained by fitting the kp model (*14*) to energies calculated by D. Vogel, P. Krüger, and J. Pollmann [*Phys. Rev. B* **54**, 5495 (1996)] and by taking β(ZnMnO) = β(ZnMnSe).
27. T. Dietl, H. Ohno, F. Matsukura, J. Cibert, D. Ferrand, data not shown.
28. K. Kim, W. L. R. Lambrecht, B. Segall, M. van Schilfgaarde, *Phys. Rev. B* **56**, 7363 (1997).

29. The work at Tohoku University was supported by the Japan Society for the Promotion of Science and by the Ministry of Education, Japan.

19 October 1999; accepted 10 December 1999

Ambipolar Pentacene Field-Effect Transistors and Inverters

J. H. Schön,* S. Berg, Ch. Kloc, B. Batlogg

Organic field-effect transistors based on pentacene single crystals, prepared with an amorphous aluminum oxide gate insulator, are capable of ambipolar operation and can be used for the preparation of complementary inverter circuits. The field-effect mobilities of carriers in these transistors increase from 2.7 and 1.7 square centimeters per volt per second at room temperature up to 1200 and 320 square centimeters per volt per second at low temperatures for hole and electron transport, respectively, following a power-law dependence. The possible simplification of the fabrication process of complementary logic circuits with these transistors, together with the high carrier mobilities, may be seen as another step toward applications of plastic electronics.

Organic thin-film field-effect transistors (FETs) have been studied extensively throughout the last decade, and tremendous progress in performance of these devices has been achieved (*1–4*). Among these organic materials, pentacene has been found to have the highest mobilities for hole transport (p channel) (*5*, *6*). State-of-the-art organic thin-film transistors reach performances similar to those of devices prepared from hydrogenated amorphous silicon (a-Si:H), with mobilities around 1 $cm^2 V^{-1} s^{-1}$ and on/off ratios surpassing 10^6, and with the use of high–dielectric constant gate insulators, operating voltages as low as 5 V can be achieved (*7*). These accomplishments demonstrate that the use of organic electronic devices may become feasible and desirable in areas in which large area coverage, mechanical flexibility, low-temperature processing, and overall low cost are required. Potential applications include low-end data storage, such as identification tags or smart cards (*8*), and even switching devices for active displays (*9*), especially because the integration of organic FETs and organic light-emitting diodes into smart pixels has been demonstrated (*9–11*). However, organic FETs have worked only as unipolar devices in accumulation or depletion, never in inversion. To exploit advantages of complementary logic, such as low-power dissipation, good noise margins, robust operation, and ease of circuit design, two different organic materials have to be used. The different semiconductors can be embedded into one heterostructure device (*12*, *13*) or into many separate devices (*14–17*), leading to all-organic digital circuits. The limitation of charge transport by only one carrier type is generally ascribed to effective trapping of the other carrier in the material itself as well as at the interface to the gate dielectric (*12*, *13*). Therefore, the use of ultrapure, high-quality materials seems to be a prerequisite to overcome this limitation.

Here, we report on organic FETs based on pentacene single crystals working as ambipolar devices both in accumulation (p type) and inversion (n type). High-purity pentacene single crystals were grown by physical vapor transport in a stream of hydrogen (*18*). Space-charge–limited current measurements (*19*) revealed trap concentrations (for holes) and acceptor densities as low as 10^{13} and 10^{11} cm^{-3}, respectively. Gold source and drain contacts (thickness of 50 nm) were evaporated through a shadow mask, defining a channel length between 25 and 50 μm and a width of 500 to 1500 μm. Al_2O_3 was deposited as gate dielectric layer by radio frequency–magnetron sputtering (capacitance $C_i \approx$ 30 nF cm^{-2}; thickness of 250 nm). Finally, the gate electrode (thickness of 100 nm) was prepared by thermal evaporation of gold (Fig. 1).

Typical device characteristics at room temperature of a pentacene single-crystal FET (Fig. 2) show the device working in both accumulation and inversion modes. The device operation of organic transistors is well described by standard FET equations (*20*), as previously shown (*7*). For accumulation (hole transport), the mobility is 2.7 $cm^2 V^{-1} s^{-1}$, and the on/off ratio at 10 V is 10^9. Typical threshold voltages are in the range of −1 V. In combination with the steep subthreshold slope of 200 meV per decade (Fig. 3), this low threshold voltage indicates the high quality of the pentacene single crystal as well as the pentacene-Al_2O_3 interface. An electron mobility of 1.7 $cm^2 V^{-1} s^{-1}$ and an on/off ratio of 10^8 are measured for operation in inversion. The higher threshold voltage of about 5 V reveals a higher density of traps for electrons than for holes. Nevertheless, n-channel transport can be obtained in pentacene devices. The observed field-effect mobility is similar to previous time-of-flight mobilities measured on related compounds such as naphtalene or anthracene (*21*).

Because no organic material has to be patterned, the use of ambipolar devices can substantially simplify the fabrication of complementary metal oxide semiconductor (CMOS)–

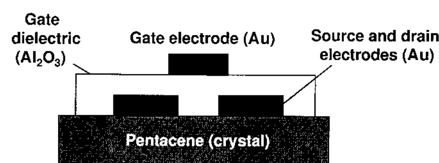

Fig. 1. Schematic structure of the FETs based on single crystalline pentacene. Gold and Al_2O_3 were used as electrode and gate insulator materials, respectively.

Bell Laboratories, Lucent Technologies, Mountain Avenue, Murray Hill, NJ 07974, USA.

*To whom correspondence should be addressed. E-mail: hendrik@lucent.com